

HOW LOUD CAN SCHWARZSCHILD BLACK HOLES RING?

JANUSZ KARKOWSKI, EDWARD MALEC

M. Smoluchowski Institute of Physics, Jagellonian University
Reymonta 4, 30-059 Kraków, Poland

AND ZDOBYŚLAW ŚWIERCZYŃSKI

Department of Computer Science and Computer Methods
Pedagogical University of Cracow
Podchorążych 1, 30-084 Kraków, Poland

(Received August 14, 2002)

A numerical procedure is described for the maximization of the energy diffusion due to the backscattering of the gravitational radiation. The obtained maxima are solutions dominated by low frequency waves. They give rise to robust gravitational ringing, with amplitudes of the order of the original signal.

PACS numbers: 04.20.-q, 04.30.Nk, 04.40.-b, 95.30.Sf

1. Motivation

The detection of gravitational radiation by the first generation of laser interferometers requires from theorists and numericists developing of the so-called templates for the Gravitational Waves (GW) produced by binary Black Holes (BH) [1,2]. That can be done for the inspiral of BH while there are significant problems as it concerns the merger phase of BH [3], where no numerical data are available as yet. In this context the next, ringing phase, of the collapse of binary BH is interesting because GW produced during this evolution period are independent to a degree on the details of its preceding history. Numerical simulations demonstrate that irrespective of the initial data, during some “intermediate” time the outgoing GW are dominated by a (fundamental) Quasinormal Mode (QM) [4], whose oscillation period and the damping coefficient depend only on characteristics of the final black hole. It is not clear, however, how energetic [5] are the QM and how big is the

ringing amplitude. The full answer to this question would require detailed information on the former evolution of the system, which is not available at present. This paper aims at finding “upper limits”, that is identifying the most favourable situations for ringing and comparing their strength — amplitudes and the energy content — with the initial energy and amplitudes. The amplitudes of strongest ringing modes are of the order of the amplitudes of GW that generate them.

2. Extremizing the diffused energy

A. Prerequisites. The space-time geometry is defined by a line element,

$$ds^2 = - \left(1 - \frac{2m}{R} \right) dt^2 + \frac{1}{1 - \frac{2m}{R}} dR^2 + R^2 d\Omega^2, \quad (1)$$

where t is a time coordinate, R is the areal radius and $d\Omega^2 = d\theta^2 + \sin^2\theta d\phi^2$ is the line element on the unit sphere, $0 \leq \phi < 2\pi$ and $0 \leq \theta \leq \pi$. The Newtonian gravitational constant G , and c , the velocity of light are put equal to 1.

We will study the propagation of polar modes Ψ of the quadrupole GW in a Schwarzschild background; they are ruled by the Zerilli equation [6]

$$(-\partial_t^2 + \partial_{r^*}^2)\Psi = V\Psi. \quad (2)$$

Here $\eta_R = 1 - 2m/R$, $V(R) = 6\eta_R^2 \frac{1}{R^2} + \eta_R \frac{63m^2(1+\frac{m}{R})}{2R^4(1+\frac{3m}{2R})^2}$ and $r^* = R + 2m \ln(\frac{R}{2m} - 1)$.

There exists a positive conserved energy E [7]; its quasilocal contribution coming from a region of a Cauchy hypersurface Σ_t exterior to a sphere of radius R reads

$$E(R, t) = 2\pi \int_R^\infty dr \rho(r, t). \quad (3)$$

Here ρ is the reduced energy density, $\rho = ((\partial_t\Psi)^2 + (\partial_{r^*}\Psi)^2 + V\Psi^2)/\eta_R$. The initial data Ψ and $\partial_t\Psi$ are assumed to be purely outgoing, smooth and to be nonzero outside a sphere of a radius $a > 2m$. Thus ρ is smooth and vanishes inside the sphere of radius a .

Let $\tilde{\Gamma}_{(R,t)}$ be an outgoing null geodesic that originates at (R, t) . By $\tilde{\Gamma}_{(R_0,t_0),(R,t)}$ will be understood a segment of $\tilde{\Gamma}_{(R_0,t_0)}$ ending at (R, t) . A straightforward calculation shows that the rate of the energy change along $\tilde{\Gamma}_{(R,0)}$ is given by

$$(\partial_t + \partial_{r^*})E(R, t) = -2\pi \left[(\partial_t\Psi + \partial_{r^*}\Psi)^2 + V\Psi^2 \right]. \quad (4)$$

Thus $E(R, t) = E(a, 0) - 2\pi \int_0^t dt \left[(\partial_t \Psi + \partial_{r^*} \Psi)^2 + V \Psi^2 \right]$, where the integral is done along $\tilde{\Gamma}_{(a,0),(R,t)}$. Some of the energy can diffuse inward due to the scattering off the curvature of the spacetime [9]. In the limiting case when the integration contour coincides with $\tilde{\Gamma}_{(a,0)}$, the energy limit $E_B(a, 0) = \lim_{t \rightarrow \infty} E(R(t), t)$ is the analogue of the Bondi mass. We will define the diffused energy as $\delta E_a = E(a, 0) - E_B(a, 0)$. Our aim is to find initial data, that maximize the **diffusion parameter** $\kappa \equiv \delta E_a / E(a, 0)$ for a sample of a 's. Let us remark that, from our experience, the computational time is proportional to the square $(a/(2m))^2$; therefore the maximization procedure would not be feasible in the case $a \gg 2m$. Fortunately, it is known from analytic estimates, that for big a 's the diffusion is negligible, since $\kappa < C(2m/a)^2$ (where C is of the order of 10) [10, 11]. Therefore, it suffices to focus on the range of relatively small distances — a being of the order of the Schwarzschild radius $2m$ — and in that case the numerical methods appear to be efficient.

B. Method. It is advantageous to search a solution of Eq. (2) in the form of $\Psi = \tilde{\Psi} + \delta$ [10]. Here $\tilde{\Psi}$ is a known function that is constructed from initial data while δ is the unknown part of the sought solution. In explicit terms

$$\tilde{\Psi} \equiv \Psi_0(r^* - t) + \frac{\Psi_1(r^* - t)}{R} + \frac{\Psi_2(r^* - t)}{R^2}, \quad (5)$$

where $\Psi_i(r^* - t)$, $i = 0, 1, 2$ fulfill the relations $\partial_t \Psi_1 = 3\Psi_0$ and $\partial_t \Psi_2 = \Psi_1 - m\partial_t \Psi_1$. $\tilde{\Psi}$ solves the Zerilli equation in Minkowski space-time ($m = 0$), in which case it represents a purely outgoing radiation. The function δ satisfies the equation

$$(-\partial_t^2 + \partial_{r^*}^2)\delta = V\delta + (V - 6\frac{\eta_R^2}{R^2}) \left(\Psi_0 + \frac{\Psi_1}{R} + \frac{\Psi_2}{R^2} \right) + \frac{2m\eta_R}{R^4} \left[-3\Psi_1 + 2\frac{\Psi_2}{R} \right], \quad (6)$$

with initial data $\delta = \partial_t \delta = 0$ at $t = 0$.

Eq. (5) and the relations between functions Ψ_i imply that initial data Ψ and $\partial_t \Psi$ are entirely determined by the specification of Ψ_0 . Ψ_0 in turn is determined (in a region outside the cone defined by $\tilde{\Gamma}_a$) by choosing $\partial_t \Psi_0$ (with $\partial_t \Psi_0|_a = 0$) in an interval $(r^*(a), \infty)$ and $\Psi_0 = 0$ for $R = a$. We have found that the numerical calculations can be significantly facilitated if the following procedure is applied. First, expand $\partial_t \Psi_0$ in an n -element Chebyshev polynomial basis (f_i) [8]; one has

$$\partial_t \Psi_0(r^*, t = 0) = \sum_{i=1}^n C_i f_i(r^*). \quad (7)$$

The initial energy becomes in this basis quadratic in C_k , $E(a, R, t = 0) \equiv 2\pi \int_a^R dr \rho(r, 0) = \sum_{i,k=1}^n B_{ik}(a, R) C_i C_k$. Second, let $\Psi_{f_k}(r^*, t)$ be a solution of (2) with initial data being defined by $f_k(r^*)$. Obviously $\Psi_{f_k}(r^*, t)$ depends only on the initial data within the null past cone with the apex at $(r^*(a), t)$. Then the solution of Eq. (2) reads

$$\Psi(r^*, t) = \sum_{i=1}^n C_i \Psi_{f_i}(r^*, t). \quad (8)$$

Let $R_1 = R(r^* = t + r^*(a))$ and $R_2 = R(r^* = 2t + r^*(a))$. The diffused energy (through $\tilde{\Gamma}_{(a,0),(R_1,t)}$) is of the form

$$\delta E_a(R, t) = \sum_{i,k=1}^n A_{ik}(a, R) C_i C_k. \quad (9)$$

The quadratic form $\delta E_a(t, R_1)$ is nonnegative; since $E(a, R, t = 0)$ is positive, the two forms can be simultaneously diagonalized. The task of comparing the extremal ratio of δE_a and $E(a, R, t = 0)$ can be reduced to the search of the maximal eigenvalue of the generalised eigenvalue problem $AX = \lambda BX$. That has been accomplished with the use of the fast EISPACK [12] package. The typical step used in numerics was $\Delta = 0.02$ and n was of the order of one thousand, depending (weakly) on the size of the initial support.

C. Extremal initial data. Below the mass m has been normalized to unity. The method described above consists in comparing local energy expressions — the energy diffused through a segment $\tilde{\Gamma}_{(a,0),(R_1,t)}$ is compared with the energy content inside the region $a \leq R \leq R_2$ of the initial hypersurface. Fixing a and R_2 , one finds $\partial_t \Psi_0^{R_2}$ (the upper index is put here in order to stress the local character of the procedure) and, through (5), initial values of the locally extremizing solution Ψ^{R_2} . With the increase of R_2 , while keeping a fixed, the function $\partial_t \Psi_0^{R_2}$ changes. In the limit one obtains the sought extremizing solution, $\Psi = \lim_{R_2 \rightarrow \infty} \Psi^{R_2}$. In the numerical practice the integration region must be finite.

Fig. 1 shows the initial profile $\partial_t \Psi_0$ for $a = 2.1$ and for various R_2 . The dependence of $\partial_t \Psi_0$ on R_2 suggests that $\lim_{R_2 \rightarrow \infty} \partial_t \Psi_0^{R_2} \approx 0$ outside some region of compact support. The parameter κ was extremized in that class of initial data which is characterized by the vanishing of $\partial_t \Psi_0$ outside some bounded region. Therefore, the chosen Ψ_0 bears on an asymptotically constant value [13]. Fig. 2 shows initial profiles of $\partial_t \Psi_0$ for $a = 2.1$, $a = 3$ and $a = 4$.

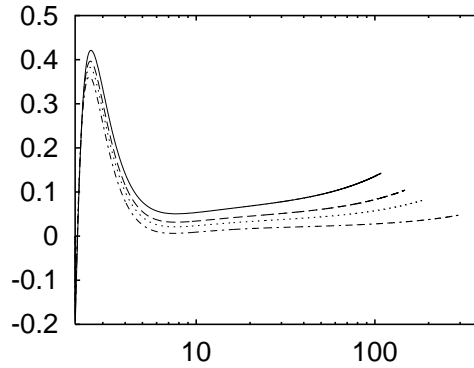


Fig. 1. Function $\partial_t \Psi_0$ in dependence on R_2 . The abscissa (R -axis) is in the (decimal) logarithmic scale. Here $a = 2.1$; solid line, broken line and dotted line correspond to $r^*(R_2) = r^*(2.1) + 6000$, $r^*(R_2) = r^*(2.1) + 8000$ and $r^*(R_2) = r^*(2.1) + 10000$, respectively. Dot-dashed line depicts the case with $r^*(R_2) = r^*(2.1) + 16000$.

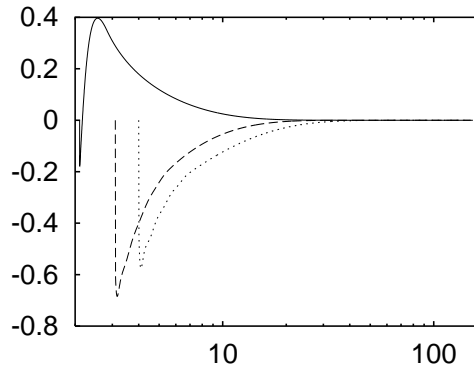


Fig. 2. Function $\partial_t \Psi_0$ for various values of a . The abscissa (R -axis) is in the (decimal) logarithmic scale. Solid line, broken line and dotted line correspond to $a = 2.1$, $a = 3$ and $a = 4$, respectively.

The obtained extremizing initial data have a **finite** total energy. Fig. 3 shows initial energy profiles for $a = 2.1$, $a = 3$ and $a = 4$. It is interesting to notice how efficient is the backscatter — κ ranges from c. 90% ($a = 2.1$) and c. 16 % ($a = 3$) to c. 4% ($a = 4$). Notice also that the region with the largest contribution to the initial energy widens with the increase of a .

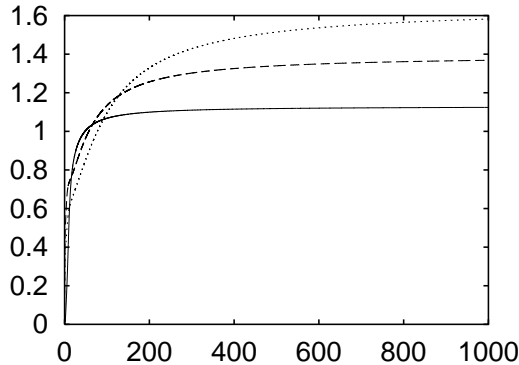


Fig. 3. Initial energy $E(R) \equiv E(a, 0) - E(R, 0)$ (y -axis) as a function of $r^* - r^*(a)$ for $a = 2.1$ (solid line), $a = 3$ (broken line) and $a = 4$ (dotted line).

3. Evolving extremal initial data

A. Ringing is loud. Our primary aim is to find initial data that give the strongest possible ringing. QM are evidently born by a subclass of multiple backscattering (see an explanation in [14]). The diffused energy δE_a bounds the energies of QM, the tail term and also of the radiation falling to a black hole. While we do not have analytic estimates of the shares of the particular contributing terms in δE_a , it is obvious that configurations with large κ have some room for robust oscillations. For that reason, instead of obeying the commonly used method of *trial and error*, we study GW defined by the **extremal initial data**. In the numerical calculations we use the splitting $\Psi = \tilde{\Psi} + \delta$ (see Sec II.B), since the numerics is then more precise.

Fig. 4 presents the radiation corresponding to the $a = 2.1$, $a = 3$ and $a = 4$ initial pulses as seen by an “observer” situated at $r_o^* = 280 + r^*(a)$. The $x = 0$ point of the abscissa corresponds to the moment of time $t = 280$. This train of initial data that moves with the speed of light is seen earlier ($t < 280$) and it lies to the right from $x = 0$. To the left from $x = 0$ we have $t > 280$; in the absence of the backscattering there would be no signal at all. Notice that in the cases $a = 2.1$ and $a = 3$ the amplitude of the strongest ringing mode is about one third of the amplitude of the original radiation, as represented by the function $\tilde{\Psi}$. The amplitude of the strongest ringing mode decreases with the increase of a — that is when the initial pulse is moved away from the horizon — but in all cases it is of the order of the initial amplitude.

B. Birth and death of ringing modes. QM boil down predominantly in the potential valley $2 < R < R_{\text{cr}} \approx 3.1$, where the maximal point R_{cr} is defined by $\partial_R V|_{R_{\text{cr}}} = 0$. Their complex frequencies carry information

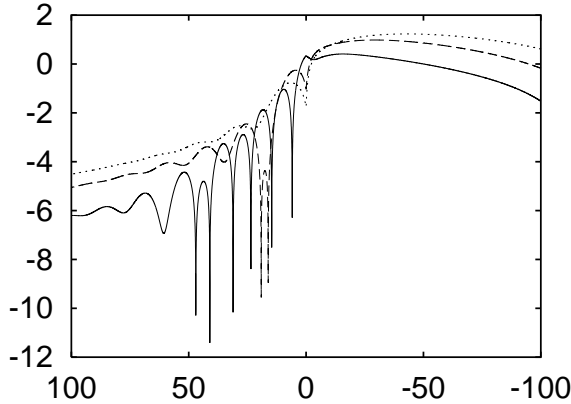


Fig. 4. Temporal dependence of $\ln |\Psi|$ (y - axis), as observed at $r_o^* = r^*(a) + 280$. Solid line, broken line and dotted line correspond to $a = 2.1$, $a = 3$ and $a = 4$, respectively.

about the curvature of the background geometry in this region. This is why the characteristic features of the ringing modes — the period and the damping coefficient of the dominant mode — do not depend on initial data. Let us point out, however, that the amplitudes of the QM depend on the frequency profile and amplitudes of initial data. We examined QM in various observation points. Fig. 5 (with $a = 4$) shows clearly that the number of nodes in a radiation pulse decreases with the distance. At the same time the

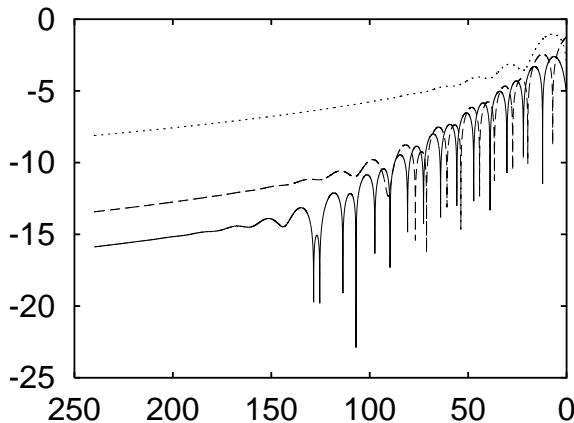


Fig. 5. Backscattered radiation (values $\ln |\Psi|$ put on y - axis), $a = 4$, as seen by an observer located at $r_o^* = 1 + r^*(4)$ (solid line), $r_o^* = 10 + r^*(4)$ (broken line) and $r_o^* = 100 + r^*(4)$ (dotted line).

dominant oscillations survive and they have the same character (but their amplitude can significantly increase) while the tail part extends.

Fig. 5 shows that there are many oscillations at $r_o^* = r^*(4) + 1$, which gradually die when the observation point is moved away — only one node is seen at $r^* = 280$ (Fig. 4). This observation that we make is probably novel in the literature, but its explanation can be standard, within the scenario described in [14].

4. Conclusions

We have found initial data that correspond to maximal values of the diffusion parameter κ ; we believe that these are optimal data for having strong QM. The largest amplitudes of QM constitute a fraction (c. 1/3) of the largest amplitude within the main pulse of the radiation. Our earlier experience [15] in numerics suggests that the effect of the backscatter depends (fixing the distance a) mostly on the frequency, and that if the dominant frequency is low (as compared to $1/m$), then the diffusion parameter κ does not depend strongly on details of the profile of initial data. This would imply that in the real collapse the ringing can be perhaps less vigorous than above, but still of interest, with amplitudes smaller by perhaps one order than those of the main pulse of GW. Similar conclusions concerning the strength of QM are valid also for the axial quadrupole GW and for the dipole electromagnetic waves [17]. The main difference between the polar and axial perturbations is that polar QM are stronger and they seem to be more “generic”, in a sense that will be explained elsewhere [17]. The same analysis can be done for higher GW multipoles.

Referring to a specific case of collapse of BH, we want to stress the following. Our results can be applied to the head-on collision of two spinless BH. If one uses the close approximation limit [16], then the outgoing part of a radiation that was produced during the earlier phases, the merger and the inspiral, should be interpreted as our initial data. If these initial data are close to “maximal”, in a sense used earlier, then the ringing amplitudes could be of the order of GW created during the coalescence of BH.

This work was partially supported by the Polish State Committee for Scientific Research (KBN) grant no 2PO3B 006 23.

REFERENCES

- [1] C. Cutler *et al.*, *Phys. Rev. Lett.* **70**, 2984 (1993).
- [2] T. Damour, R.R. Iyer, B.S. Sathyaprakash, Detecting Binary Black Holes With Efficient and Reliable Templates in Gravitational Waves — A challenge to Theoretical Physics, Proceedings of Trieste conference, 2000.
- [3] P.R. Brady, J.D.E. Creighton, K.S. Thorne, *Phys. Rev.* **D58**, 061501 (1998).
- [4] See the following review papers and references therein: K.D. Kokkotas, B. Schmidt, *Living Rev. Rel.* **2**, 2 (1999); H.P. Nollert, *Class. Quantum Grav.* **16**, R159 (1999).
- [5] H.P. Nollert, R. Price, *J. Math. Phys.* **40**, 980 (1999).
- [6] F. Zerilli, *Phys. Rev. Lett.* **24**, 737 (1970); *Phys. Rev.* **D2**, 2141 (1970).
- [7] The energy density ρ is probably proportional to the Landau–Lifschitz type energy density of gravitational waves, up to a divergence term. Here the energy $E(R, t)$ can be regarded as an subsidiary quantity that appears to be useful in constructing the strongest QM.
- [8] We tried also the Legendre polynomials, sin and cos trigonometric bases and wavelets, but the numerics was fastest with the Chebyshev polynomials.
- [9] There exists a vast literature on the backscatter — see below and references therein: C. Misner, K. Thorne, J.A. Wheeler, *Gravitation*, Freeman, San Francisco 1973; J. Bicak, *Gen. Rel. Grav.* **3**, 331 (1972); R. Price, *Phys. Rev.* **D5**, 2419 (1972); J.M. Bardeen, W.H. Press, *J. Math. Phys.* **14**, 7 (1973); B. Mashhoon, *Phys. Rev.* **D7**, 2807 (1973); L. Blanchet, G. Schäfer, *Class. Quantum Grav.* **10**, 2699 (1993); E. Malec, *Phys. Rev.* **D62**, 084034 (2000); S. Hod, *Phys. Rev.* **D66**, 024001 (2002).
- [10] E. Malec, G. Schäfer, *Phys. Rev.* **D64**, 044012 (2001).
- [11] J. Karkowski, E. Malec, Z. Świerczyński, *Acta Phys. Pol. B* **32**, 3593 (2001).
- [12] This can be found in www.netlib.org
- [13] Ψ_0 itself can be set to zero through, say, introducing a damping factor outside some $R_M \gg 2m$. This modification would not change our conclusions and we keep a nonzero asymptotic value of Ψ_0 since it is more convenient in doing numerics.
- [14] E.S.C. Ching *et al.*, *Phys. Rev. Lett.* **74**, 2414 (1995); *Phys. Rev.* **D52**, 2118 (1995).
- [15] J. Karkowski, E. Malec, Z. Świerczyński, *Class. Quantum Grav.* **19**, 953 (2002).
- [16] R.H. Price, J. Pullin, *Phys. Rev. Lett.* **72**, 3297 (1994).
- [17] J. Karkowski, K. Roszkowski, Z. Świerczyński, E. Malec, [gr-qc/0210041](http://arxiv.org/abs/gr-qc/0210041).